Classification of Matrix-Product Unitaries with Symmetries

Zongping Gong,[1,2] Christoph Sünderhauf,[2,3] Norbert Schuch,[2,3] and J. Ignacio Cirac[2,3]
[1]*Department of Physics, University of Tokyo, 7-3-1 Hongo, Bunkyo-ku, Tokyo 113-0033, Japan*
[2]*Max-Planck-Institut für Quantenoptik, Hans-Kopfermann-Straße 1, D-85748 Garching, Germany*
[3]*Munich Center for Quantum Science and Technology, Schellingstraße 4, D-80799 München, Germany*

(Received 31 December 2018; accepted 21 February 2020; published 13 March 2020)

We prove that matrix-product unitaries with on-site unitary symmetries are *completely* classified by the (chiral) index and the cohomology class of the symmetry group G, provided that we can add trivial and symmetric ancillas with arbitrary on-site representations of G. If the representations in both system and ancillas are fixed to be the same, we can define symmetry-protected indices (SPIs) which quantify the imbalance in the transport associated to each group element and greatly refines the classification. These SPIs are stable against disorder and measurable in interferometric experiments. Our results lead to a systematic construction of two-dimensional Floquet symmetry-protected topological phases beyond the standard classification, and thus shed new light on understanding nonequilibrium phases of quantum matter.

DOI: 10.1103/PhysRevLett.124.100402

Introduction.—Classification of topological phases of matter is a central issue in modern condensed matter physics [1]. Particular recent interest is attracted by the classification of topological systems far from thermal equilibrium [2–15]. This tendency is largely driven by the remarkable experimental developments in atomic, molecular and optical physics, which have opened up unprecedented flexibility for controlling and probing quantum many-body dynamics [16–21]. Moreover, understanding nonequilibrium phases of matter *per se* is of fundamental theoretical importance in extending the conventional paradigm of statistical mechanics to the largely unexplored nonequilibrium regime [22–24].

For equilibrium interacting systems, the arguably most well-understood classification is that of one-dimensional (1D) bosonic symmetry-protected topological (SPT) phases [25–28] as ground states of gapped local Hamiltonians with symmetries. These 1D SPT phases are well described by the matrix-product states (MPSs) [29–32], and are completely classified by the second cohomology group [33–36], provided that the symmetries are not spontaneously broken. An analogous minimal setting in the nonequilibrium context is the classification of matrix-product unitaries (MPUs) [36–39], which have been shown to be equivalent to quantum cellular automata [38]. They efficiently approximate finite-time 1D dynamics generated by local Hamiltonians [40]. While an MPU can be regarded as an MPS with an enlarged local Hilbert space, the classification of MPUs can be very different from that of MPSs due to the unitarity requirement. Indeed, without symmetry protection, MPSs can always be continuously deformed into product states, while MPUs are classified by the (chiral) index quantized as the logarithm of a rational number [37–39,41]. Efforts have also been made to classify 1D SPT many-body-localized (MBL) phases, and the result turns out to be the same as that of ground-state SPT MPSs [42].

In stark contrast to the case of MPSs, the problem of classifying MPUs commuting with a local symmetry operation stays unsolved. In this Letter, we address this problem for general on-site unitary symmetries forming a finite group G. First, we allow adding arbitrary symmetric ancillas (identities) with arbitrary on-site representations of G. We prove that the combination of the index and the second cohomology class *completely* classifies all the MPUs with given symmetries. This actually proves a conjecture raised by Hastings [43] for quantum cellular automata. Second, we allow ancillas only with the same symmetry representation as the original system. Here, we unveil a series of quantized symmetry-protected indices (SPIs). Nonzero SPIs quantify an imbalance of the left and right transport of each group element in the Heisenberg picture. We identify an observable signature of SPIs as the asymmetries in the two edges of symmetry-string operators evolved by the MPU, and propose an interferometry experiment for probing the SPIs relative to the index.

Our results have direct implications in the classification of Floquet SPT phases [44]. Given a 2D Floquet system with boundary in the MBL regime, its edge dynamics is well described by an MPU [37]. Here, we construct a class of 2D Floquet systems with edge MPUs characterized by nontrivial SPIs, and provide a unified picture for understanding the edge dynamics of 2D intrinsic Floquet SPT phases as symmetry-charge pumps.

Matrix-product unitaries.—We are interested in 1D quantum dynamics that keep locality, i.e., the unitaries U's that map any operator O supported on a finite region into $U^\dagger O U$ supported on another finite region. In particular, we wish to classify all possible U that can continuously be deformed into each other by keeping locality, which defines different dynamical phases. According to Ref. [38], this allows us to use MPUs, which we define in the following.

An MPU of length L is a unitary operator $U^{(L)}: (\mathbb{C}^d)^{\otimes L} \to (\mathbb{C}^d)^{\otimes L}$ generated by a rank-four tensor $\mathcal{U}$:

$$U^{(L)} = \sum_{i_1,\ldots,i_L,j_1,\ldots,j_L} \mathrm{Tr}(\mathcal{U}_{i_1 j_1} \ldots \mathcal{U}_{i_L j_L}) |i_1,\ldots,i_L\rangle\langle j_1,\ldots,j_L|. \tag{1}$$

The dimension D of the matrices $\mathcal{U}_{ij}$ is called bond dimension. After blocking k, at most D^4 times (combining multiple physical indices into one index), $\mathcal{U} \to \mathcal{U}_k$ is termed *simple* and $U^{(L)}$ acquires the standard form

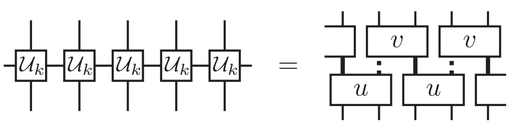
(2)

in terms of unitaries $u: (\mathbb{C}^{d^k})^{\otimes 2} \to \mathbb{C}^l \otimes \mathbb{C}^r$ and $v: \mathbb{C}^r \otimes \mathbb{C}^l \to (\mathbb{C}^{d^k})^{\otimes 2}$. We apply operators in the graphical notation from bottom to top. The unitaries are unique up to gauge transformations $u \to (X^\dagger \otimes Y^\dagger)u$, $v \to v(Y \otimes X)$, where d is the local Hilbert-space dimension before blocking, $X \in \mathrm{U}(l)$ and $Y \in \mathrm{U}(r)$. Conversely, two arbitrary unitaries u and v generate a MPU, possibly with the unit cell doubled.

We will focus our attention on G-symmetric MPUs which commute with a unitary representation ρ_g of the finite group G, $[\rho_g^{\otimes L}, U^{(L)}] = 0$. Henceforth, we omit the length L due to the translation-invariance of MPUs and assume the standard form. Although we assume translation invariance throughout the letter, all the topological indicators we unveil can be shown to be stable against disorder [45]. The essential physics behind the stability is the locality-preserving constraint, which is obviously satisfied by the standard form (2) even if u and v are position dependent.

Equivalence and complete classification.—We classify the MPUs according to

Definition 1.—(Equivalence) Two G-symmetric MPUs U_0 and U_1 are equivalent if we allow for blocking (i.e., treat multiple sites as a single site), and the addition of local ancillas with the identity operator, such that the MPUs can then be continuously connected within the manifold of symmetric MPUs.

Here, by adding local ancillas to an MPU U, we mean that we take the enlarged MPU $U' = U \otimes \mathbb{1}_{\mathrm{a}}^{\otimes L}$ on $(\mathbb{C}^d \otimes \mathbb{C}^{d_{\mathrm{a}}})^{\otimes L}$, and consider the representation $\rho'_g = \rho_g \otimes \sigma_g$, where σ can be an *arbitrary* representation of G on $\mathbb{C}^{d_{\mathrm{a}}}$.

MPUs can be considered as MPSs by bunching the two physical indices of each tensor into one. Thus, G-symmetric MPUs can be associated to a cohomology class in $H^2[G, \mathrm{U}(1)]$ [51]. However, the fact that they are unitary gives extra restrictions. In order to analyze these restrictions, we employ the standard form (2) and note that, due to the gauge redundancy, the action of the symmetry on the building blocks consists of two projective representations x_g and y_g:

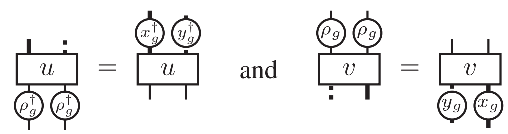
(3)

Both x_g and y_g^* belong to the same cohomology class as the associated MPS [45].

The index [38,39,41] of the MPU is defined as

$$\mathrm{ind} \equiv \frac{1}{2}\log\frac{r}{l} = \frac{1}{2}\log\frac{\mathrm{Tr} y_e}{\mathrm{Tr} x_e} \tag{4}$$

for the identity $e \in G$; it captures the imbalance of right- and left-moving information. Both index and cohomology class are stable under blocking and additive under tensoring as well as composition of MPUs [45].

As Hastings conjectured [43], equivalent phases are indeed completely classified by index and cohomology:

Theorem 1.—(Equivalence) Two symmetric MPUs U_0 and U_1 with the same or different symmetry representations are equivalent if and only if they share the same indices and same cohomology classes.

Note that the necessity of the same indices was shown by Cirac *et al.* [38]; that of same cohomology classes follows from Ref. [34], just as for MPS. We then only have to construct an explicit path that continuously connects U_0 with U_1. This turns out to be always possible after a symmetrization of the on-site symmetry representations of U_0 and U_1 and a regularization through attaching ancillas with regular representations [45].

Examples of MPUs with nontrivial cohomology classes are already found in Refs. [53,54] as the edge dynamics of 2D intrinsic Floquet SPT phases [55]. Initialized as a symmetric state, a nontrivial 1D edge evolves from one SPT phase into another after each Floquet period, reminiscent of the discrete time crystals that toggle between different symmetry-broken phases [56–59]. In the tensor-network picture, we can understand this "topological discrete time-crystalline oscillation" from the virtual level—when a symmetric MPS is evolved by a symmetric MPU, their cohomology classes simply sum up [see Fig. 1(a)].

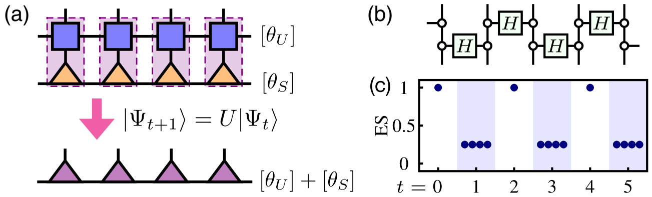

FIG. 1. (a) G-symmetric MPS evolved by a G-symmetric MPU with the cohomology classes summing up. (b) $\mathbb{Z}_2 \times \mathbb{Z}_2$-symmetric MPU in the nontrivial cohomology class. Here $\circ$ is the delta tensor and H is the Hadamard matrix. (c) Stroboscopic dynamics of the entanglement spectrum (ES) governed by (b) starting from a symmetric product state.

To diagnose this phenomenon, we may trace the stroboscopic evolution of the entanglement spectrum [10,12,13], which is experimentally accessible by many-body-state tomography [60] or interferometric measurement [61]. For the $G = \mathbb{Z}_n \times \mathbb{Z}_n$ SPT MPU corresponding to the generator of $H^2[G, U(1)] = \mathbb{Z}_n$ [53], starting from a symmetric trivial state, we will obtain (at least) $[n/gcd(n,t)]^2$-fold degeneracy in the entanglement spectrum after t time steps [45]. See Figs. 1(b) and 1(c) for the simplest case $n = 2$. More general examples with nontrivial cohomology classes are available in the Supplemental Material [45].

Strong equivalence and symmetry-protected indices.—In real physical systems with symmetries, the representation is usually determined by the microscopic details and cannot be changed freely. This motivates us to ask how the classification will be modified if the representation is fixed. Forbidding arbitrary representations for the ancillas in Definition 1 leads to

Definition 2.—(Strong equivalence) Two G-symmetric MPUs U_0 and U_1 are strongly equivalent if (i) their on-site representations are (generally different) powers of a single fixed representation ρ of G and (ii) they can be continuously connected within the manifold of symmetric MPUs upon blocking and/or adding identities as ancillas with representation ρ.

If ρ is regular, we will return to Theorem 1. Otherwise, there is at least one $g \neq e$ with character $\chi_g \equiv \mathrm{Tr}\rho_g \neq 0$. In this case, the notion of strong equivalence refines the phase structure beyond Theorem 1, as revealed by the SPIs which are the natural generalization of the index (4) to other group elements:

Definition 3.—(Symmetry protected index) Given a G-symmetric MPU U for which we can determine x_g and y_g from a standard form, the SPI with respect to $g \in G$ with $\chi_g \neq 0$ is defined as

$$\mathrm{ind}_g \equiv \frac{1}{2}\log\left|\frac{\mathrm{Tr}y_g}{\mathrm{Tr}x_g}\right|. \tag{5}$$

Given a blocking number k, the SPI is well defined since the absolute value removes the phase ambiguity and the trace is gauge invariant. Moreover, we can show that, just like $\mathrm{ind} = \mathrm{ind}_e$ [38], ind_g is invariant under blocking and additive under tensoring and composition [45].

We further claim that the SPI is a topological invariant for strong equivalence. Recall that ind_g does not rely on blocking and is obviously invariant if we add identities with the fixed representation. Moreover, it can be shown that ind_g is continuous and stays discretized during a continuous deformation [45]. Therefore, the SPI is a quantizied topological invariant, implying

Theorem 2.—Two symmetric, strongly equivalent MPUs share the same SPI for all group elements with $\chi_g \neq 0$.

The contraposition of Theorem 2 allows us to use SPIs to distinguish topologically different MPUs. For cyclic groups $G = \mathbb{Z}_n$ with $n \geq 3$, the minimal nontrivial example is the bilayer SWAP circuit of qubits [38], where a single site contains two qubits and $\rho_{1_{\mathbb{Z}_n}} = \mathbb{1} \otimes Z_{\omega_n}$ ($1_{\mathbb{Z}_n}$: generator of $\mathbb{Z}_n$) and $Z_{\omega_n} \equiv |0\rangle\langle 0| + e^{2\pi i/n}|1\rangle\langle 1|$ [see Fig. 2(d)]. We can check that $x_{1_{\mathbb{Z}_n}} = \mathbb{1}^{\otimes 2}$ and $y_{1_{\mathbb{Z}_n}} = Z_{\omega_n}^{\otimes 2}$, leading to $\mathrm{ind}_{1_{\mathbb{Z}_n}} = \log|\cos(\pi/n)| \neq 0$, which is sufficient to rule out the *strong* equivalence between the bilayer SWAP circuit and the identity. However, having $\mathrm{ind} = 0$ and trivial cohomology, it is still equivalent to the identity. While the SPI therefore allows for an enriched classification for strong equivalence, the classification provided by Theorem 2 is *not* complete [45].

Physical implication and experimental probing of SPIs.—Similar to the cohomology character, the SPI (5) is defined on the virtual level, so its physical meaning is not clear at first glance. Having in mind that SPT phases with nontrivial cohomology classes usually exhibit exotic edge physics [62], we are naturally led to think about a similar situation for SPIs, which depend on g. In fact, we can consider a sufficiently long string operator $\rho_g^{\otimes N}$ evolved by the MPU and show that the g-string operator will almost stay unchanged, except that near the left and right edges two $2k$-site unitaries L_g and R_g emerge [see Fig. 2(a)]. These two unitaries on the physical level are related to x_g and y_g on the virtual level via $L_g = u^\dagger(x_e \otimes y_g)u$ and $R_g = u^\dagger(x_g \otimes y_e)u$, leading to

$$\mathrm{ind}_g - \mathrm{ind} = \frac{1}{2}\log\left|\frac{\mathrm{Tr}L_g}{\mathrm{Tr}R_g}\right|. \tag{6}$$

It is now clear from Eq. (6) that ind_g gives a measure of the edge imbalance in the g-string operator evolved by the MPU.

Equation (6) also opens up the possibility for practically measuring the SPI relative to the index. Note that $\mathrm{Tr}L_g\mathrm{Tr}R_g = d^{2k}\chi_g^{2k}$; it is sufficient to measure either $|\mathrm{Tr}L_g|$ or $|\mathrm{Tr}R_g|$. This problem can be simplified into how to measure $|\mathrm{Tr}U_A|$ for a subsystem unitary U_A embedded in $U = U_A \otimes U_B$, where the Hilbert-space dimension d_B of subsystem B can be much larger than d_A, that of subsystem A. Combining $|\mathrm{Tr}U_A|^2 = d_B^{-1}\mathrm{Tr}_B[\mathrm{Tr}_A U \mathrm{Tr}_A U^\dagger]$ with the

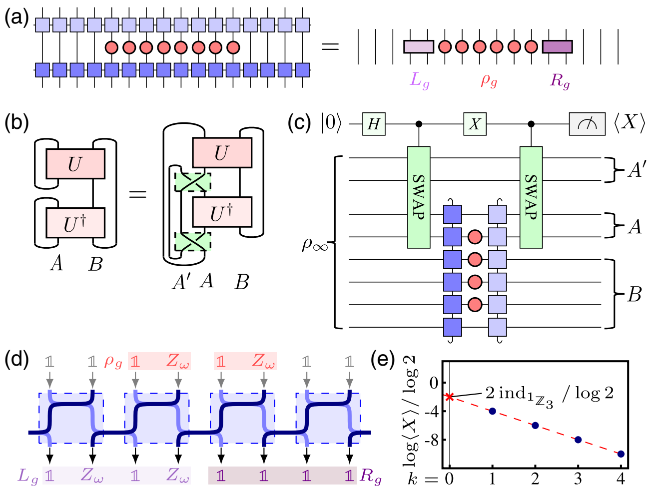

FIG. 2. (a) Symmetry string operator evolved by a symmetric MPU. Only the left and right edges are modified into L_g and R_g, respectively. (b) Tensor-network representation of $\mathrm{Tr}_B[\mathrm{Tr}_A U \mathrm{Tr}_A U^\dagger] = \mathrm{Tr}[U\mathbb{S}U^\dagger\mathbb{S}]$, where $\mathbb{S}$ (green rectangles) is the SWAP operator between subsystem A and its copy A'. (c) Interferometric approach to probing the relative SPI (6). Initially, the qubit is set to be $|0\rangle$ while the remaining part is prepared as the infinite-temperature state ρ_∞. Here H is the Hadamard gate and the controlled-SWAP gates read $U_{\mathrm{CS}} = |0\rangle\langle 0| \otimes \mathbb{1}_{A'A} + |1\rangle\langle 1| \otimes \mathbb{S}$. The final expectation value $\langle X\rangle$ of the qubit is related to $|\mathrm{Tr}L_g|$ and thus the relative SPI. (d) Bilayer SWAP circuit subject to $\mathbb{Z}_n$ symmetry. (e) SPI of (d) with respect to $1_{\mathbb{Z}_{n=3}}$ determined by linear fitting (7).

identity in Fig. 2(b), we obtain $|\mathrm{Tr}U_A|^2 = d_A^2 \mathrm{Tr}[U\mathbb{S}\rho_\infty U^\dagger \mathbb{S}]$, where $\mathbb{S}$ is the SWAP operator acting on A and a copy A' and $\rho_\infty \equiv d_A^{-2} d_B^{-1} \mathbb{1}_{A'AB}$ is the infinite-temperature state of the entire system including A'. Since eventually we rewrite $|\mathrm{Tr}U_A|^2$ into the form of a Loschmidt echo, we can measure it by means of the standard interferometric approach [63–66].

We sketch out the experimental scheme in Fig. 2(c), where an auxiliary qubit is introduced and either of two controlled-SWAP gates consists of $2k$ two-site ones acting on a region A near the left domain wall and its copy A'. By measuring the final expectation value $\langle X\rangle$ for the Pauli X of the auxiliary qubit, we can determine the relative SPI from

$$\mathrm{ind}_g - \mathrm{ind} = \frac{1}{2}\log\langle X\rangle + k\log\frac{d}{|\chi_g|}. \qquad (7)$$

If d and χ_g are unknown, we are still able to measure $\langle X\rangle$ with increasing length $2k$ of A and then extract $\mathrm{ind}_g - \mathrm{ind}$ from a linear fitting. See Fig. 2(e) for the example of the bilayer SWAP circuit subject to $\mathbb{Z}_3$ symmetry.

General parent Floquet systems as symmetry-charge pumps.—Recalling the relation between MPUs and Floquet systems, the (strong) equivalence between MPUs are *necessary* for the (strong) equivalence between the corresponding G-symmetric 2D MBL Floquet systems—they are continuously connected without crossing a delocalization point [37,53,54]. This is because MBL implies a spatial factorization of the bulk Floquet unitary and its separation from the boundary unitary, which is 1D, locality preserving, and thus well described by an MPU [37]. A continuous deformation of the Floquet system thus gives rise to that of the edge MPU. Conversely, two inequivalent MPUs *sufficiently* distinguish their parent Floquet systems.

It is thus natural to ask whether an MPU with nontrivial SPIs can be embedded into a parent Floquet system, just like those with nontrivial indices [37] and cohomology classes [53,54]. Since topologically different MPUs distinguish different MBL parent Floquet systems, the embeddability would imply a new class of 2D SPT Floquet phases characterized by SPIs. We answer in the affirmative by giving a general construction shown and explained in Fig. 3(a), whose bulk is trivial and thus many-body localizable [67], while the edge dynamics is governed by an MPU generated by u and $v = u^\dagger \mathbb{S}_\mathrm{v}$, where $\mathbb{S}_\mathrm{v}$ exchanges the virtual Hilbert spaces $\mathbb{C}^l$ and $\mathbb{C}^r$. This construction is inspired by the standard form (2) and the four-step SWAP model [37,68,69]—we compose two four-step SWAP processes, one on the left virtual Hilbert spaces and pulled back by u, and the other on the physical level.

The above general construction of parent Floquet systems in turn gives a simple symmetry-charge-pump picture for topological MPUs. Here a G-symmetry charge refers to a Hilbert space on which G acts as a linear (integer charge) or projective representation (fractional charge). These charges can fuse or split following the fusion rules set

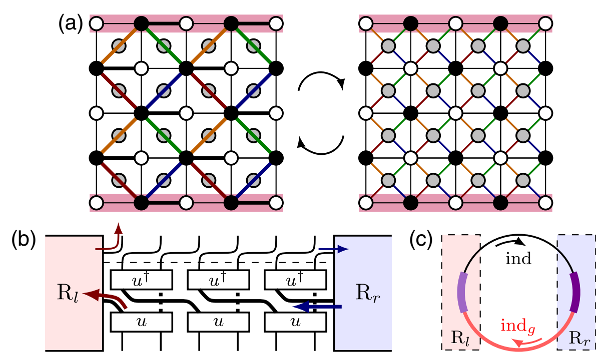

FIG. 3. (a) 2D Floquet system with a trivial bulk and a nontrivial edge dynamics (shaded in magenta) governed by an MPU. The open (periodic) boundary condition is imposed to the vertical (horizontal) direction. In the first (left panel) and second (right panel) half period, we apply u-conjugated (thick black bonds) SWAP gates (thick color bonds) and physical-level SWAP gates (color bonds) sequentially as red → blue → green → orange. (b) MPU segment as a symmetry-charge pump that transfers q_o from R_l to R_r and q_x from R_r to R_l. The circuits above and below the dashed line are generated by the left and right panel in (a). (c) Edge imbalance (light and dark purple) in an evolved g-string operator (pink) from current imbalance (6).

by the group structure. With the physical and the left virtual charge in the standard form denoted as $q_\varrho \equiv kq_\rho$ and q_x [70], an MPU segment coupled to two symmetry reservoirs $\mathrm{R}_{l,r}$ right translates q_ϱ and left translates q_x [see Fig. 3(b)]. In fact, the cohomology class and the SPIs (including the index) are all characters of the net symmetry-charge current $q_\varrho - q_x$. This picture unifies all the related previous works as special situations, such as $G = \{e\}$ [37,69] and $\mathrm{Tr}x_g = \mathrm{Tr}\varrho_g = \delta_{ge}\dim\varrho$ [53,54]. Remarkably, this picture gives an intuition into Eq. (6): We regard two equally long segments centered at the edges of a g-string operator as $R_{l,r}$, which are connected by two pumps with inputs g and e [see Fig. 3(c)]. We can then interpret Eq. (6) as an equation of continuity, with the left- and right-hand sides being the current and the change of charge, respectively. There is a factor $\frac{1}{2}$ since a net flow of charge q causes $2q$ charge imbalance.

Summary and outlook.—We have focused on the classification problem of symmetric MPUs, where the symmetry representation can be arbitrary or fixed. In the former case, we achieve a complete classification based on the index and the cohomology class. In the latter case, we unveil a set of experimentally accessible SPIs that enrich the classification and lead to the discovery of a new class of 2D Floquet SPT phases. However, the complete classification in the latter case stays an open problem, which we leave for future work. Other directions for future studies include the generalization to antiunitary [38] and continuous symmetries, fermionic systems [72], and higher dimensions [73]. Since both SPIs and cohomology classes apply to inhomogeneous unitaries, it would also be interesting to study the impact of topology on information scrambling in random circuits [74–80].

We acknowledge M. Ueda, K. Shiozaki, M. Furuta, M. Sato, D. T. Stephen, H. Tasaki, and H. Katsura for valuable discussions. This project has received funding from the European Research Council (ERC) under the European Union's Horizon 2020 research and innovation programme through the ERC Starting Grant WASCOSYS (No. 636201) and the ERC Advanced Grant QENOCOBA (No. 742102), and from the Deutsche Forschungsgemeinschaft (DFG) under Germany's Excellence Strategy (EXC-2111–390814868). Z. G. acknowledges support from the University of Tokyo through the Graduate Research Abroad in Science Program (GRASP) and the Max-Planck-Institut für Quantenoptik for hospitality, where this work was completed.

[1] C.-K. Chiu, J. C. Y. Teo, A. P. Schnyder, and S. Ryu, Rev. Mod. Phys. **88**, 035005 (2016).
[2] T. Kitagawa, E. Berg, M. Rudner, and E. Demler, Phys. Rev. B **82**, 235114 (2010).
[3] C.-E. Bardyn, M. A. Baranov, C. V. Kraus, E. Rico, A. İmamoğlu, P. Zoller, and S. Diehl, New J. Phys. **15**, 085001 (2013).
[4] D. V. Else and C. Nayak, Phys. Rev. B **93**, 201103(R) (2016).
[5] C. W. von Keyserlingk and S. L. Sondhi, Phys. Rev. B **93**, 245145 (2016).
[6] A. C. Potter, T. Morimoto, and A. Vishwanath, Phys. Rev. X **6**, 041001 (2016).
[7] R. Roy and F. Harper, Phys. Rev. B **96**, 155118 (2017).
[8] S. Yao, Z. Yan, and Z. Wang, Phys. Rev. B **96**, 195303 (2017).
[9] Z. Gong, Y. Ashida, K. Kawabata, K. Takasan, S. Higashikawa, and M. Ueda, Phys. Rev. X **8**, 031079 (2018).
[10] Z. Gong and M. Ueda, Phys. Rev. Lett. **121**, 250601 (2018).
[11] S. Higashikawa, M. Nakagawa, and M. Ueda, Phys. Rev. Lett. **123**, 066403 (2019).
[12] M. McGinley and N. R. Cooper, Phys. Rev. Lett. **121**, 090401 (2018).
[13] M. McGinley and N. R. Cooper, Phys. Rev. B **99**, 075148 (2019).
[14] M. McGinley and N. R. Cooper, Phys. Rev. Research **1**, 033204 (2019).
[15] A. Coser and D. Pérez-García, Quantum **3**, 174 (2019).
[16] J. T. Barreiro, M. Müller, P. Schindler, D. Nigg, T. Monz, M. Chwalla, M. Hennrich, C. F. Roos, P. Zoller, and R. Blatt, Nature (London) **470**, 486 (2011).
[17] P. Schindler, M. Müller, D. Nigg, J. T. Barreiro, E. A. Martinez, M. Hennrich, T. Monz, S. Diehl, P. Zoller, and R. Blatt, Nat. Phys. **9**, 361 (2013).
[18] S. Choi, J. Choi, R. Landig, G. Kucsko, H. Zhou, J. Isoya, F. Jelezko, S. Onoda, H. Sumiya, V. Khemani, C. von Keyserlingk, N. Y. Yao, E. Demler, and M. D. Lukin, Nature (London) **543**, 221 (2017).
[19] H. Bernien, S. Schwartz, A. Keesling, H. Levine, A. Omran, H. Pichler, S. Choi, A. S. Zibrov, M. Endres, M. Greiner, V. Vuletić, and M. D. Lukin, Nature (London) **551**, 579 (2017).
[20] J. Zhang, P. W. Hess, A. Kyprianidis, P. Becker, A. Lee, J. Smith, G. Pagano, I.-D. Potirniche, A. C. Potter, A. Vishwanath, N. Y. Yao, and C. Monroe, Nature (London) **543**, 217 (2017).
[21] J. Zhang, G. Pagano, P. W. Hess, A. Kyprianidis, P. Becker, H. Kaplan, A. V. Gorshkov, Z.-X. Gong, and C. Monroe, Nature (London) **551**, 601 (2017).
[22] J. Eisert, M. Friesdorf, and C. Gogolin, Nat. Phys. **11**, 124 (2015).
[23] R. Nandkishore and D. A. Huse, Annu. Rev. Condens. Matter Phys. **6**, 15 (2015).
[24] R. Moessner and S. L. Sondhi, Nat. Phys. **13**, 424 (2017).
[25] F. D. M. Haldane, Phys. Rev. Lett. **50**, 1153 (1983).
[26] I. Affleck, T. Kennedy, E. H. Lieb, and H. Tasaki, Phys. Rev. Lett. **59**, 799 (1987).
[27] Z.-C. Gu and X.-G. Wen, Phys. Rev. B **80**, 155131 (2009).
[28] F. Pollmann, A. M. Turner, E. Berg, and M. Oshikawa, Phys. Rev. B **81**, 064439 (2010).
[29] M. Fannes, B. Nachtergaele, and R. F. Werner, Commun. Math. Phys. **144**, 443 (1992).
[30] F. Verstraete and J. I. Cirac, Phys. Rev. B **73**, 094423 (2006).
[31] D. Pérez-García, F. Verstraete, M. M. Wolf, and J. I. Cirac, Quantum Inf. Comput. **7**, 401 (2007).

[32] F. Verstraete, V. Murg, and J. I. Cirac, Adv. Phys. **57**, 143 (2008).
[33] D. Pérez-García, M. M. Wolf, M. Sanz, F. Verstraete, and J. I. Cirac, Phys. Rev. Lett. **100**, 167202 (2008).
[34] N. Schuch, D. Pérez-García, and I. Cirac, Phys. Rev. B **84**, 165139 (2011).
[35] X. Chen, Z.-C. Gu, and X.-G. Wen, Phys. Rev. B **83**, 035107 (2011).
[36] X. Chen, Z.-C. Gu, and X.-G. Wen, Phys. Rev. B **84**, 235128 (2011).
[37] H. C. Po, L. Fidkowski, T. Morimoto, A. C. Potter, and A. Vishwanath, Phys. Rev. X **6**, 041070 (2016).
[38] J. I. Cirac, D. Pérez-García, N. Schuch, and F. Verstraete, J. Stat. Mech. (**2017**) 083105.
[39] M. B. Şahinoğlu, S. K. Shukla, F. Bi, and X. Chen, Phys. Rev. B **98**, 245122 (2018).
[40] T. J. Osborne, Phys. Rev. Lett. **97**, 157202 (2006).
[41] D. Gross, V. Nesme, H. Vogts, and R. F. Werner, Commun. Math. Phys. **310**, 419 (2012).
[42] A. Chan and T. B. Wahl, arXiv:1808.05656.
[43] M. B. Hastings, Phys. Rev. B **88**, 165114 (2013).
[44] F. Harper, R. Roy, M. S. Rudner, and S. Sondhi, Annu. Rev. Condens. Matter Phys. **11** (2020).
[45] See Supplemental Material at http://link.aps.org/supplemental/10.1103/PhysRevLett.124.100402 for details, which includes Refs. [46–50].
[46] J.-P. Serre, *Linear Representations of Finite Groups* (Springer, New York, 1977).
[47] R. Dijkgraaf and E. Witten, Commun. Math. Phys. **129**, 393 (1990).
[48] M. Christandl, arXiv:quant-ph/0604183.
[49] G. Vidal, Phys. Rev. Lett. **98**, 070201 (2007).
[50] X. Chen, Z.-C. Gu, Z.-X. Liu, and X.-G. Wen, Phys. Rev. B **87**, 155114 (2013).
[51] This differs sharply from the setting where MPUs themselves form a linear representation of G, a situation related to equilibrium 2D SPT states classified by $H^3[G, \mathrm{U}(1)]$ [43,52].
[52] X. Chen, Z.-X. Liu, and X.-G. Wen, Phys. Rev. B **84**, 235141 (2011).
[53] A. C. Potter and T. Morimoto, Phys. Rev. B **95**, 155126 (2017).
[54] R. Roy and F. Harper, Phys. Rev. B **95**, 195128 (2017).
[55] By intrinsic, we mean that they have no equilibrium counterparts and correspond to $H^2[G, \mathrm{U}(1)]$ part in the cohomology classification $H^3[\mathbb{Z}\times G, \mathrm{U}(1)] = H^3[G, \mathrm{U}(1)] \times H^2[G, \mathrm{U}(1)]$ [4].
[56] V. Khemani, A. Lazarides, R. Moessner, and S. L. Sondhi, Phys. Rev. Lett. **116**, 250401 (2016).
[57] D. V. Else, B. Bauer, and C. Nayak, Phys. Rev. Lett. **117**, 090402 (2016).
[58] C. W. von Keyserlingk and S. L. Sondhi, Phys. Rev. B **93**, 245146 (2016).
[59] N. Y. Yao, A. C. Potter, I.-D. Potirniche, and A. Vishwanath, Phys. Rev. Lett. **118**, 030401 (2017).
[60] B. P. Lanyon, C. Maier, M. Holzäpfel, T. Baumgratz, C. Hempel, P. Jurcevic, I. Dhand, A. S. Buyskikh, A. J. Daley, M. Cramer, M. B. Plenio, R. Blatt, and C. F. Roos, Nat. Phys. **13**, 1158 (2017).
[61] H. Pichler, G. Zhu, A. Seif, P. Zoller, and M. Hafezi, Phys. Rev. X **6**, 041033 (2016).
[62] D. V. Else and C. Nayak, Phys. Rev. B **90**, 235137 (2014).
[63] R. Dorner, S. R. Clark, L. Heaney, R. Fazio, J. Goold, and V. Vedral, Phys. Rev. Lett. **110**, 230601 (2013).
[64] B. Swingle, G. Bentsen, M. Schleier-Smith, and P. Hayden, Phys. Rev. A **94**, 040302(R) (2016).
[65] G. Zhu, M. Hafezi, and T. Grover, Phys. Rev. A **94**, 062329 (2016).
[66] N. Y. Yao, F. Grusdt, B. Swingle, M. D. Lukin, D. M. Stamper-Kurn, J. E. Moore, and E. A. Demler, arXiv:1607.01801.
[67] A. C. Potter and A. Vishwanath, arXiv:1506.00592.
[68] M. S. Rudner, N. H. Lindner, E. Berg, and M. Levin, Phys. Rev. X **3**, 031005 (2013).
[69] F. Harper and R. Roy, Phys. Rev. Lett. **118**, 115301 (2017).
[70] Technically speaking, according to the character theory of projective representations [71], q_x is specified by a 2-cocycle $\theta: G\times G \to 2\pi\mathbb{R}/\mathbb{Z}$ and a vector $\eta: G \to \mathbb{C}\cup\{-\infty\}$, $\eta(g) = \log \mathrm{Tr} x_g$ (we take log to make q additive) subject to the gauge transformation $\theta(g,h) \to \theta(g,h) + \tau(g) + \tau(h) - \tau(gh)$, $\eta(g) \to \eta(g) + i\tau(g)$ for $\forall\, \tau: G \to 2\pi\mathbb{R}/\mathbb{Z}$.
[71] C. Cheng, Linear Algebra Appl. **469**, 230 (2015).
[72] L. Fidkowski, H. C. Po, A. C. Potter, and A. Vishwanath, Phys. Rev. B **99**, 085115 (2019).
[73] J. Haah, L. Fidkowski, and M. B. Hastings, arXiv:1812.01625.
[74] C. W. von Keyserlingk, T. Rakovszky, F. Pollmann, and S. L. Sondhi, Phys. Rev. X **8**, 021013 (2018).
[75] T. Rakovszky, F. Pollmann, and C. W. von Keyserlingk, Phys. Rev. X **8**, 031058 (2018).
[76] A. Nahum, S. Vijay, and J. Haah, Phys. Rev. X **8**, 021014 (2018).
[77] V. Khemani, A. Vishwanath, and D. A. Huse, Phys. Rev. X **8**, 031057 (2018).
[78] C. Sünderhauf, D. Pérez-García, D. A. Huse, N. Schuch, and J. I. Cirac, Phys. Rev. B **98**, 134204 (2018).
[79] A. Chan, A. De Luca, and J. T. Chalker, Phys. Rev. Lett. **121**, 060601 (2018).
[80] A. Chan, A. De Luca, and J. T. Chalker, Phys. Rev. X **8**, 041019 (2018).